FIFTEENTH NATIONAL RADIO SCIENCE CONFERENCE
Feb. 24-26 , 1998 , Helwan , Cairo , Egypt.

Thermal-Stress-Induced Birefringence in Panda and Bow-Tie Optical Fibers

Moustafa H. Aly*, M. Sami A. Abouelwafa, and Mohamed M. Keshk

Department Engineering Mathematics and Physics
Faculty of Engineering, University of Alexandria
* Member of the Optical Society of America

ABSTRACT:

In this paper, a thermoelastic potential method is introduced to calculate the stress distribution in mechanically homogeneous birefringent fibers. Two kinds of such fibers; namely panda and bow-tie fibers, are studied and their birefringence is calculated. Stress distribution of bow-tie fiber is compared with that obtained from the finite element method showing a fair agreement. Results show that a higher degree of birefringence can be obtained by increasing stress applying zone area, decreasing the distance of this zone from the core and to some extent by increasing the cladding area.

I. INTRODUCTION

In most applications, an optical fiber is a means for transmitting signals in the form of optical power with pulse-code or intensity modulation; the signal is detected by a photodiode that is insensitive to optical polarization or phase. Even a single-mode fiber is not truly a single mode since it can support two degenerate modes that are dominantly polarized in two orthogonal directions [1]. Under ideal conditions of perfect cylindrical geometry and isotropic material, a mode excited with its polarization in the x direction would not couple to the mode with the y-orthogonal polarization [2]. In practice, small departures from cylindrical geometry or small fluctuations in material anisotropy result in a mixing of the two polarization states.

In high-birefringent (HB) fibers, the linear polarization state is forcedly maintained. A large amount of birefringence, B, is introduced intentionally in these fibers through design modifications so that small random birefringence fluctuations do not affect significantly the light polarization. A high-birefringent fiber requires $B > 10^{-5}$ and a value better than 10^{-4} is a minimum for perfect polarization maintenance [3].

The total modal birefringence, B, is composed of the geometrical component, B_G, induced by the shape difference of the core, the self-stress component, B_{So}, induced by the thermal expansion difference of the asymmetrical core, and the outer stress-component, B_S, induced by the stress-applying zone (SAZ) which will be our main subject [4].

The determination of the polarization properties of the fiber requires the knowledge of mechanical stress distribution in the cross section of the fiber. The function of this stress is to change the intrinsic refractive index of the glass. The stress calculation in a birefrengent fiber is usually achieved by the finite element method [5]. This method, however, requires an elaborate formulation of the elements over the whole fiber cross section for a given structure and the solution of a large system of equations. These render the method inflexible to use and time consuming in computation. In this study, we use the theory for

transforming the problem of determining the stress distribution into a potential problem in which the Poisson's equation is solved.

II. THEORY

The assumptions of the adopted method can be summarized as: (1) Since the potential, in general, is a linear scalar quantity, the principle of superposition holds. Consequently, the total stress in the fiber is obtained by adding the contributions from individual stress-producing components [6]. (2) Because different optical refractive indices of the fiber regions are obtained through the use of a doping technique, the mechanical properties of the core, the cladding, and the SAZs all remain nearly the same [5]. (3) As a consequence of the doping process, the thermal expansion coefficients in these three regions are completely different and will be symbolized as α_1, α_2 and α_3 for core, cladding and SAZ materials.

In accordance with the work of Bernat [7], the calculation of elastic stresses is reduced to the calculation of the potential χ ($= \phi + F$), the sum of the thermoelastic potential ϕ and the elastic potential F. These potentials satisfy:

$$\nabla^2\phi = \frac{1+\nu}{1-\nu}\alpha T \quad , \tag{1}$$

$$\nabla^4 F(r,\theta) = 0 \quad , \tag{2}$$

where ν is Poisson's ratio and T is the difference between the ambient temperature and the melting temperature of the glass. Airy stress function ,F(r , θ) is given as [7]:

$$F(r,\theta) = a_0 + b_0 r^2 + \sum_{n=1}^{\infty}(a_n r^n + b_n r^{n+2})\cos n\theta \quad , \tag{3}$$

where the coefficients a_n and b_n are to be determined from boundary conditions.

As mentioned before, to get the birefringence one must start with getting the radial stress component, σ_r, the circumferential stress component, σ_θ, and the shear stress component, $\sigma_{r\theta}$, which can be obtained from the following system of equations [7]:

$$\sigma_r = \frac{-E}{1+\nu}\frac{1}{r}\left[\frac{\partial\chi}{\partial r} + \frac{\partial^2\chi}{r\partial\theta^2}\right] \quad , \tag{4}$$

$$\sigma_\theta = \frac{-E}{1+\nu}\frac{\partial^2\chi}{\partial r^2} \quad , \tag{5}$$

$$\sigma_{r\theta} = \frac{E}{1+\nu}\frac{\partial}{\partial r}\left[\frac{1}{r}\frac{\partial\chi}{\partial\theta}\right] \quad , \tag{6}$$

where E is the Young's constant and these equations are subjected to the boundary conditions of zero radial and shear stress at cladding boundary.

According to the elastooptic theory, the stress-induced birefringence B_0 at the core center is defined as [8]:

$$B_0 = (C_2 - C_1)\left[\sigma_y(0,0) - \sigma_x(0,0)\right] \quad , \tag{7}$$

where C_1 and C_2 are the elastooptical coefficients of the fiber material, while σ_x and σ_y are the stress components in the x and y directions (obtained from the transformation of Eqs. 4, 5 and 6 to the Cartesian system). Clearly, the average birefringence over the cross-sectional area, A, of the fiber is:

$$B_{av} = \frac{(C_2 - C_1)}{A} \iint_A \left[\sigma_y(r,\theta) - \sigma_x(r,\theta)\right] r \, d\theta \, dr \quad , \qquad (8)$$

In order to obtain the V number dependence of the modal birefringence, the overlap integral between the optical field ψ (r, θ, V) of the HE_{11} mode and the stress distribution is necessary. The effective birefringence B_e can be evaluated as [9]:

$$B_e = (C_2 - C_1) \frac{\int_0^{2\pi}\int_0^{\infty} \left[\sigma_y(r,\theta) - \sigma_x(r,\theta)\right] \psi^2(r, \theta, V)\, r \, dr \, d\theta}{\int_0^{2\pi}\int_0^{\infty} \psi^2(r, \theta, V)\, r \, dr \, d\theta} \quad , \qquad (9)$$

Panda Fiber

The structure of this fiber is shown in Fig. (1). To obtain the thermoelastic displacement potential $\phi(r, \theta)$ due to the inhomogeneity of the cylinder, the term α in Eq.(1) is replaced by $(\alpha_1 - \alpha_2)$ in the core region and by $(\alpha_3 - \alpha_2)$ in the stress producing region. The displacement potential, ϕ (r, θ) , is splitted into two potentials ($\phi = \phi_1 + \phi_3$), where ϕ_1 is the contribution due to the core and ϕ_3 is the contribution due to the stress applying zones. Then ϕ_1 and ϕ_3 satisfy Poisson's equation inside their respective regions and Laplace's equation outside those regions. These equations are given as:

$$\nabla^2 \phi_i = \frac{1+\nu}{1-\nu} (\alpha_i - \alpha_2) T = \beta_i T \, , \quad i = 1,3 \quad \text{(inside)} \quad , \qquad (10)$$

$$\nabla^2 \phi_i = 0 \quad , \quad \text{(outside)} \quad . \qquad (11)$$

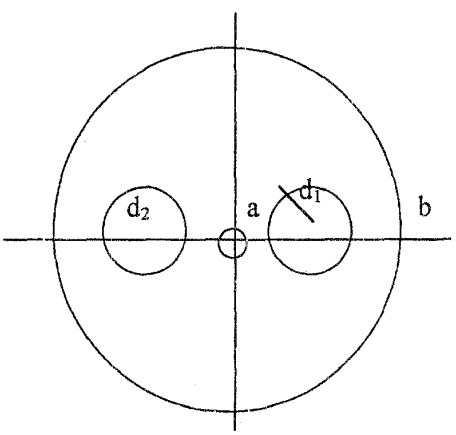

Fig. (1) Panda Fiber

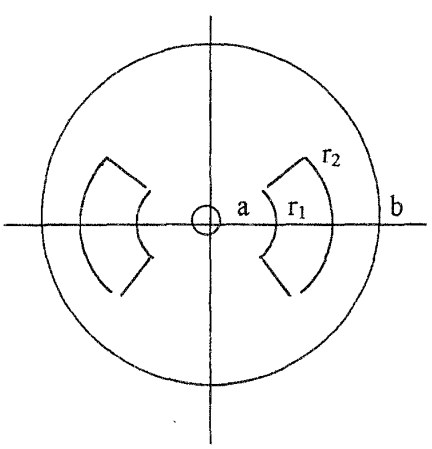

Fig. (2) Bow-Tie Fiber

Taking into account the circular symmetry, the contribution of the core is [10]:

$$\phi_1(r) = \frac{\beta_1 T}{4} r^2 + K_1 \quad , \quad r \le a$$
$$\phi_1(r) = \frac{a^2 \beta_1 T}{2} \ln r + K_2 \quad , \quad r \ge a \qquad (12)$$

where K_1 and K_2 are constants of no interest in calculating stresses since these stresses depend on the derivatives of ϕ. The potential due to each of the stress lobes can be obtained by a simple translation of coordinates, so that:

$$\phi_{3\mp} = \frac{\beta_3 T}{4}\left(r^2 \pm 2rd_2\cos\theta + d_2^2\right) + K_3 \quad , \quad \text{(inside)}$$
$$\phi_{3\mp} = \frac{\beta_3 T d_1^2}{4}\ln\left(r^2 \pm 2rd_2\cos\theta + d_2^2\right) + K_4 \quad , \quad \text{(outside)} \qquad (13)$$

where the positive sign is for the right lobe and the negative is for the left one and K_3 and K_4 are also constants of no interest.

Adding the contribution from Airy stress function given by Eq. (3) and applying the boundary conditions, stresses throughout the fiber cross section can be calculated. The stresses at any point of the fiber due to Airy stress function are obtained as:

$$\sigma_r^A = \frac{ET}{1+\nu}\left[X_1 + \frac{\beta_3 d_1^2}{b^2}X_2\right] \quad , \qquad (14)$$

$$\sigma_\theta^A = \frac{ET}{1+\nu}\left[X_1 - \frac{\beta_3 d_1^2}{b^2}X_3\right] \quad , \qquad (15)$$

$$\sigma_{r\theta}^A = \frac{-ET}{1+\nu}\frac{\beta_3 d_1^2}{b^2}X_4 \quad , \qquad (16)$$

where E is Young's modules and X_i are given as:

$$X_1 = \frac{\beta_1 a^2}{2b^2} + \frac{\beta_3 d_1^2}{b^2} \quad ,$$

$$X_{2,3} = \sum\left[(4n^2-1)\left(\frac{d_2}{b}\right)^2\left(\frac{rd_2}{b^2}\right)^{2n-2} - 2(n\mp 1)(2n+1)\left(\frac{rd_2}{b^2}\right)^{2n}\right]\cos 2n\theta \quad ,$$

$$X_4 = \sum\left[(4n^2-1)\left(\frac{d_2}{b}\right)^2\left(\frac{rd_2}{b^2}\right)^{2n-2} - 2n(2n+1)\left(\frac{rd_2}{b^2}\right)^{2n}\right]\sin 2n\theta \quad . \qquad (17)$$

Inside the core, the contribution from the displacement potential is obtained as:

$$\sigma_r^\phi = \frac{-ET}{2(1+\nu)}\left[\beta_1 + \beta_3 d_1^2\left(\frac{X_5}{X_7^2} + \frac{X_6}{X_8^2}\right)\right] \quad , \qquad (18)$$

$$\sigma_\theta^\phi = \frac{-ET}{2(1+\nu)}\left[\beta_1 + \frac{\beta_3 d_1^2}{2}\left(\frac{2X_7 - X_9^2}{X_7^2} + \frac{2X_8 - X_{10}^2}{X_8^2}\right)\right] \quad , \qquad (19)$$

$$\sigma_{r\theta}^\phi = \frac{-ET}{1+\nu}\beta_3 d_1^2 d_2\sin\theta\left[\frac{X_9}{2X_7^2} - \frac{X_{10}}{2X_8^2}\right] \quad , \qquad (20)$$

where

$$X_{5,6} = r^2 + d_2^2\cos 2\theta \mp 2rd_2\cos\theta \quad , \quad X_{7,8} = r^2 \mp 2rd_2\cos\theta + d_2^2$$
$$X_{9,10} = 2r \mp 2d_2\cos\theta \quad . \qquad (21)$$

Keeping in mind that when X has two subscripts, the first corresponds to the negative sign in the right hand side of the equation.

In the stress applying zones, the stresses due to the displacement potential are :

$$\sigma_r^\phi = \frac{-ET}{2(1+\nu)}\left(\frac{\beta_1 a^2}{r^2} + \beta_3\left[1 + d_1^2\frac{X}{Y^2}\right]\right) \quad , \qquad (22)$$

$$\sigma_{\theta}^{\phi} = \frac{ET}{2(1+\nu)}\left(\frac{\beta_1 a^2}{r^2} + \beta_3\left[-1 + d_1^2\frac{X}{Y^2}\right]\right) \quad , \tag{23}$$

$$\sigma_{r\theta}^{\phi} = \frac{ET}{1+\nu}\beta_3 d_1^2 d_2 \frac{Z\sin\theta}{Y^2} \quad , \tag{24}$$

where X, Y, and Z must be replaced by X_6, X_8 and X_{10} respectively for the right stress lobe and by X_5, X_7 and X_9 for the left stress lobe.
In the cladding region the stress distribution is obtained in the following forms:

$$\sigma_{r}^{\phi} = \frac{-ET}{2(1+\nu)}\left[\frac{\beta_1 a^2}{r^2} + \beta_3 d_1^2\left(\frac{X_5}{X_7^2} + \frac{X_6}{X_8^2}\right)\right] \quad , \tag{25}$$

$$\sigma_{\theta}^{\phi} = -\sigma_{r}^{\phi} \quad , \tag{26}$$

$$\sigma_{r\theta}^{\phi} = \frac{-ET}{1+\nu}\beta_3 d_1^2 d_2 \sin\theta\left[\frac{X_9}{2X_7^2} - \frac{X_{10}}{2X_8^2}\right] \quad , \tag{27}$$

Bow-Tie Fiber

This kind of polarization-maintaining fiber has a structure shown in Fig. (2). The potential due to the circular core is again given by Eq. (12), while the potential ϕ_3 due to the stress applying zones is found by integrating Green's function given as [10]:

$$\begin{aligned} G(r,\theta\,;\,r_0,\vartheta_0) &= \frac{\beta T}{2\pi}\ln r - \frac{\beta T}{2\pi}\sum\frac{1}{n}\left(\frac{r_0}{r}\right)^n \cos(n(\theta-\theta_0)) \quad , \quad r \succ r_0 \\ &= \frac{\beta T}{2\pi}\ln r_0 - \frac{\beta T}{2\pi}\sum\frac{1}{n}\left(\frac{r_0}{r}\right)^n \cos(n(\theta-\theta_0)) \quad . \quad r \prec r_0 \end{aligned} \tag{28}$$

Integrating Green's function, the potential due to the stress zones is :

$$\phi_3(r,\theta) = \frac{\beta_1 T}{\pi}\begin{pmatrix} \frac{\theta_1}{2}\left[r_2^2(2\ln r_2 - 1) - r_1^2(2\ln r_1 - 1)\right] \\ -\frac{1}{4}\sum\frac{r^{2n}}{n^2(n-1)}\left[\frac{1}{r_1^{2(n-1)}} - \frac{1}{r_2^{2(n-1)}}\right]\cos 2n\theta\,\sin 2\theta_1 \end{pmatrix} \quad , \quad 0 \le r \le r_1$$

$$\phi_3 = \frac{\beta_1 T}{\pi}\begin{pmatrix} -\theta_1(r_1^2\ln r - r_2^2\ln r_2) - \theta_1(r_2^2 - r^2)/2 \;-\; 1/4 \\ \sum\frac{1}{n^2}\left[\frac{2nr^2}{n^2-1} - \frac{r_1^{2(n+1)}}{(n+1)r^{2n}} - \frac{r^{2n}}{(n-1)r_2^{2(n-1)}}\right]\cos 2n\theta\,\sin 2\theta_1 \end{pmatrix} \quad , \quad r_1 \le r \le r_2$$

$$\phi_3 = \frac{\beta_1 T}{\pi}\left(\theta_1(r_2^2 - r_1^2)/r + \frac{1}{2}\sum\frac{1}{n(n+1)}\frac{r_2^{2(n+1)} - r_1^{2(n+1)}}{r^{2n+1}}\cos 2n\theta\,\sin 2\theta_1\right) \quad . \quad r_2 \le r \le b \tag{29}$$

Using Green's function and applying the boundary conditions, the stress distribution can be found. First, stresses from Airy's function is :

$$\sigma_r^A = \frac{ET}{1+\nu}\left(\frac{\beta_3\theta_1}{\pi}\left[\left(\frac{r_2}{b}\right)^2 - \left(\frac{r_1}{b}\right)^2\right] + \frac{a^2\beta_1}{2b^2} + \frac{\beta_3}{\pi}\sum(Y_1 - Y_2)Y_3Y_4\right) \quad , \tag{30}$$

$$\sigma_\theta^A = \frac{ET}{1+\nu}\left(\frac{\beta_3\theta_1}{\pi}\left[\left(\frac{r_2}{b}\right)^2 - \left(\frac{r_1}{b}\right)^2\right] + \frac{a^2\beta_1}{2b^2} - \frac{\beta_3}{\pi}\sum (Y_1 - Y_5)Y_3Y_4\right) \quad , \qquad (31)$$

$$\sigma_{r\theta}^A = -\frac{ET\beta_3}{(1+\nu)\pi}\sum (Y_1 - Y_5)Y_3 \sin 2n\theta \sin 2n\theta_1 \quad , \qquad (32)$$

where Y_1 to Y_5 are given by :

$$Y_1 = \frac{n(4n^2-1)}{2(n+1)}\left(\frac{r}{b}\right)^{2(n-1)} \quad , \quad Y_2 = \frac{(2n+1)(n-1)}{n(n+1)}\left(\frac{r}{b}\right)^{2n}$$

$$Y_3 = \left(\frac{r_2}{b}\right)^{2(n+1)} - \left(\frac{r_1}{b}\right)^{2(n+1)} \quad , \quad Y_4 = \cos 2n\theta \sin 2n\theta_1$$

$$Y_5 = \frac{2n+1}{n+1}\left(\frac{r}{b}\right)^{2n} \quad . \qquad (33)$$

The stresses due to the displacement potential are splitted into two components, the first comes from the stress applying zones and the second comes from the core contribution. Stresses from the stress zones is presented as :

$$\sigma_r^{\phi 3} = -\frac{ET\beta_3}{(1+\nu)\pi}\sum \frac{2n-1}{2n(n-1)}\left[\left(\frac{r}{r_1}\right)^{2(n-1)} - \left(\frac{r}{r_2}\right)^{2(n-1)}\right]\cos 2n\theta \sin 2n\theta_1 \quad ,$$

$$0 \le r \le r_1$$

$$= -\frac{ET\beta_3}{(1+\nu)\pi}\left(\begin{array}{l}\theta_1\left[1-\left(\frac{r_1}{r}\right)^2\right] \\ +\sum\left[\frac{(2n^2-1)}{n(n^2-1)} - \frac{2n+1}{2n(n+1)}\left(\frac{r_1}{r}\right)^{2(n+1)} - \frac{(2n-1)}{2n(n-1)}\left(\frac{r}{r_2}\right)^{2(n-1)}\right] \\ \cos 2n\theta \sin 2n\theta_1\end{array}\right) ,$$

$$r_1 \le r \le r_2$$

$$= -\frac{ET\beta_3}{(1+\nu)\pi}\left(\theta_1\frac{r_2^2 - r_1^2}{r^2} + \sum\frac{2n+1}{2n(n+1)}\frac{r_2^{2(n+1)} - r_1^{2(n+1)}}{r^{2(n+1)}}\cos 2n\theta \sin 2n\theta_1\right) .$$

$$r_2 \le r \le b \qquad (34)$$

$$\sigma_\theta^{\phi 3} = \frac{ET\beta_3}{(1+\nu)\pi}\sum \frac{2n-1}{2n(n-1)}\left[\left(\frac{r}{r_1}\right)^{2(n-1)} - \left(\frac{r}{r_2}\right)^{2(n-1)}\right]\cos 2n\theta \sin 2n\theta_1 \quad ,$$

$$0 \le r \le r_1$$

$$= \frac{ET\beta_3}{(1+\nu)\pi}\left(\theta_1\frac{r_2^2-r_1^2}{r^2}+\sum\left[\frac{1}{n(n^2-1)}-\frac{2n+1}{2(n+1)n}\left(\frac{r_1}{r}\right)^{2(n+1)}-\frac{2n-1}{2n(n-1)}\left(\frac{r}{r_2}\right)^{2(n-1)}\right]\cos 2n\theta \sin 2n\theta_1\right), \quad r_1 \le r \le r_2$$

$$= \frac{ET\beta_3}{(1+\nu)\pi}\left(\theta_1\frac{r_2^2-r_1^2}{r^2}+\sum\frac{2n+1}{2n(n+1)}\frac{r_2^{2(n+1)}-r_1^{2(n+1)}}{r^{2(n+1)}}\cos 2n\theta \sin 2n\theta_1\right), \quad r_2 \le r \le b \qquad (35)$$

$$\sigma_{r\theta}^{\phi 3} = \frac{ET\beta_3}{(1+\nu)\pi}\sum\frac{2n-1}{2n(n-1)}\left[\left(\frac{r}{r_1}\right)^{2(n-1)}-\left(\frac{r}{r_2}\right)^{2(n-1)}\right]\sin 2n\theta \sin 2n\theta_1, \quad 0 \le r \le r_1$$

$$= \frac{ET\beta_3}{(1+\nu)\pi}\sum\left[\frac{1}{n(n^2-1)}+\frac{2n+1}{2n(n+1)}\left(\frac{r_1}{r}\right)^{2(n+1)}-\frac{2n-1}{2n(n-1)}\left(\frac{r}{r_2}\right)^{2(n-1)}\right]\sin 2n\theta \sin 2n\theta_1, \quad r_1 \le r \le r_2$$

$$= -\frac{ET\beta_3}{(1+\nu)\pi}\sum\frac{2n+1}{n}\left[\left(\frac{r_2}{r}\right)^{2(n+1)}-\left(\frac{r_1}{r}\right)^{2(n+1)}\right]\sin 2n\theta \sin 2n\theta_1, \quad r_2 \le r \le b \qquad (36)$$

Finally, the stresses due to the core are obtained as:

$$\sigma_r^{\phi 1} = \frac{-ET}{1+\nu}\frac{\beta_1}{2}, \quad 0 \le r \le a$$

$$= \frac{-ET}{1+\nu}\frac{\beta_1 a^2}{2r^2}, \quad a \le r \le b \qquad (37)$$

$$\sigma_\theta^{\phi 1} = \frac{-ET}{1+\nu}\frac{\beta_1}{2}, \quad 0 \le r \le a$$

$$= \frac{ET}{1+\nu}\frac{\beta_1 a^2}{2r^2}, \quad a \le r \le b \qquad (38)$$

$$\sigma_{r\theta}^{\phi 1} = 0, \quad 0 \le r \le b \qquad (39)$$

II. RESULTS AND DISCUSSION

The method of the displacement potential, described above, has been applied for the determination of the material birefringence in a panda fiber. This fiber is supposed to have a

core, cladding and SAZ radii equal 5, 60 and 15 μm respectively [11]. The mechanical properties of the fiber are E = 7830 kg/mm^2 and ν = 0.186, while the thermal expansion coefficients of the different regions in this fiber are $\alpha_1 = 2.125\times10^{-6}$, $\alpha_2 = 5.4\times10^{-7}$ and $\alpha_3 = 1.45\times10^{-6}$ °C^{-1} [12].

Figure (3) shows the dependence of the material birefrengence on d_2, the distance from the origin to the SAZ center. Three representations of the birefringence are observed in this figure symbolized as B_0,B_{av} and B_e. The third is considered to be the most accurate over the other representations because it does not ignore the influence of wavelength dependence of the optical field. The required electric field distribution is calculated at 1.3 μm, a 0.0025 relative refractive-index difference and a value of n_1 equals 1.4516. It can be observed from Fig. (3) that birefringence decreases slightly when going towards the core boundary and has its maximum at the origin, so, the average birefringence is lower in magnitude than that at the origin. Since the effective birefringence, B_e, is an average value weighted by the square of the field, it lies between B_0 and B_{av} according to the fact that the field distribution is maximum at the origin. All the remaining curves of this study will be in terms of the average birefringence for the sake of simplicity in calculation. Figure (3) also shows the increase of the birefringence with decreasing d_2 since the influence of the SAZ increases when it comes closer to the core.

In Fig. (4), the birefringence is plotted Vs the radius of the SAZ, d_1, at different values of cladding radius, b. From this figure a direct proportionality between birefringence and both the area of the SAZ and the cladding radius can be observed.

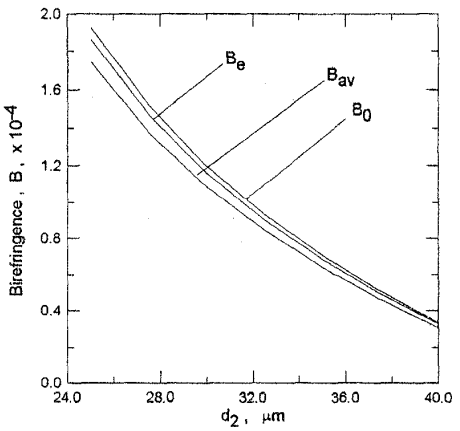

Fig. (3) The different representations of the material birefringence, in a panda fiber, as a function of d_2, the distance from the origin to the SAZ center.

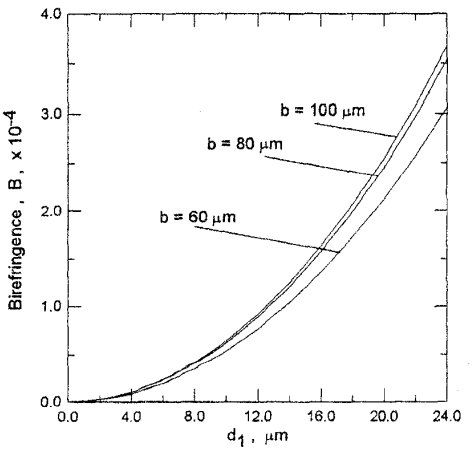

Fig. (4) The dependence of the material birefringence, in a panda fiber, on d_1, the radius of the SAZ, at different cladding radius, b, values.

The mechanical strength of optical fibers is an important factor to realize optical fiber communication systems. Although the tensile strength is not critical in conventional metallic cable technology because of the flexibility of metal, it should be fully considered in optical

fibers because of the brittleness of glass [11]. For this reason, the axial stress, σ_z , is calculated according to the following equation [13]:

$$\sigma_z = \nu(\sigma_x + \sigma_y) - E\alpha T \qquad (40)$$

In Figs. (5) and (6), the axial stress component at certain points in the fiber is plotted against α_2 and α_3. It is found from these curves that: (1) Axial stress at any point throughout the fiber cross-section are tensile (positive values), in a good agreement with the results published in Refs. [11] and [14]. (2) Average value of σ_z changes severely with α_3, but with α_2 a slight dependence is observed. (3) Maximum axial stress occurs at the center of the core, while minimum value occurs at the outer boundary of the cladding. Maximum value of σ_z is about 5 times the minimum value, and this ratio may approach 10 times in case of low α_2 values.

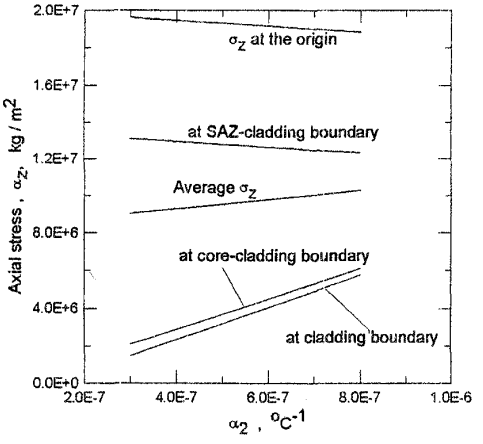

Fig. (5) The axial stress component, σ_z, at certain points, of the panda fiber, as a function of the thermal expansion coefficient of the cladding material.

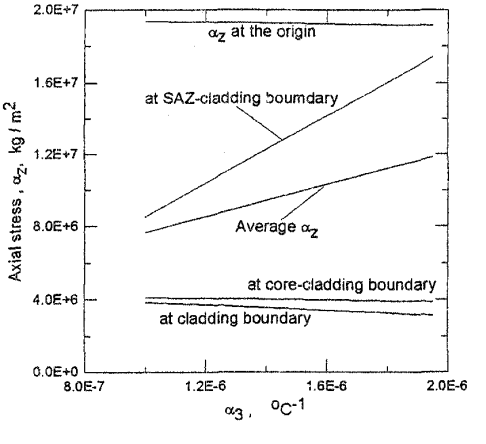

Fig. (6) The axial stress component, σ_z, at certain points, of the panda fiber, as a function of the thermal expansion coefficient of the SAZ material.

The second HB fiber of interest is the bow-tie fiber which has been the subject of many papers concerning the calculation of the thermal stresses as well as the evaluation of the birefringence of such fiber. In this study, fiber dimensions are a = 4, b = 50, r_1 = 15, and r_2 = 25 μm, where r_1, r_2 are inner and outer radii of the SAZ.

The first work in bow-tie fiber was attended by Pak L. Chu [6] who used the thermoelastic potential method. The present work, which depends on the same theory is compared with the work of Danny Wong [5] and T.V.Grattan [13] based on the point-matching method and the finite element method respectively. Figures (7) and (8) display the variation of both radial and tangential stresses with distance along x-axis. From these curves it is found that:

1- Radial stress, σ_r , and tangential stress, σ_θ , inside the core are nearly constant.
2- The radial stress along x-axis is positive in the SAZ area and increases with x in a good agreement with the results of Danny Wong [5] and in contrast with those of the earlier work of Pak [6]. On the other hand, σ_θ along x-axis in the SAZ region is relatively high and decreases with x as published in [5] and the experimental work of Ref. [14].
3- σ_r decays fairly smooth to zero as we move towards the fiber boundary along x-axis whereas σ_θ decays to some negative value. This negative tangential stress at the outer cladding indicates that the fiber is under compression.

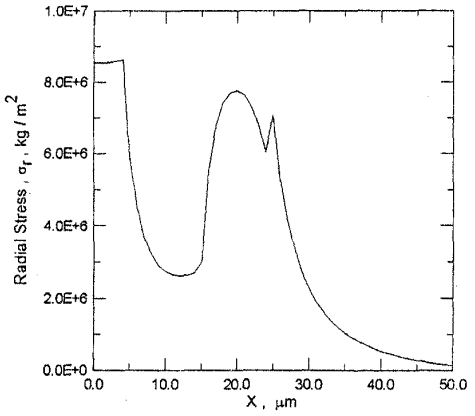

Fig. (7) Radial stress, σ_r, along x-axis in a bow-tie fiber.

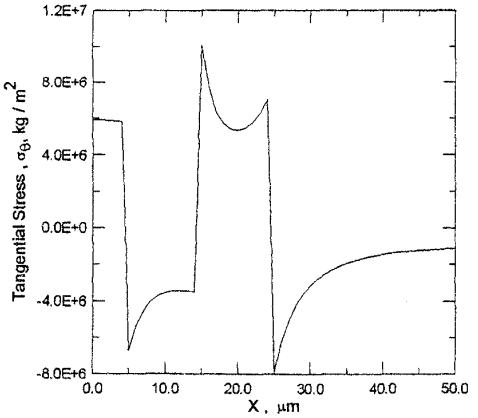

Fig. (8) Tangential stress, σ_θ, along x-axis in a bow-tie fiber.

The influence of changing r_1 on the value of B is plotted in Fig. (9). In this figure, the second curve is obtained keeping the thickness of the SAZ constant (10 μm) and the decrease in B while increasing r_1 is correct because when the SAZ moves away from the core its effect becomes weaker. In the first curve, the same inverse proportionality is seen but with a higher gradient since the decrease in B is due to two reasons, the SAZ moves away from the core and this zone becomes thinner.

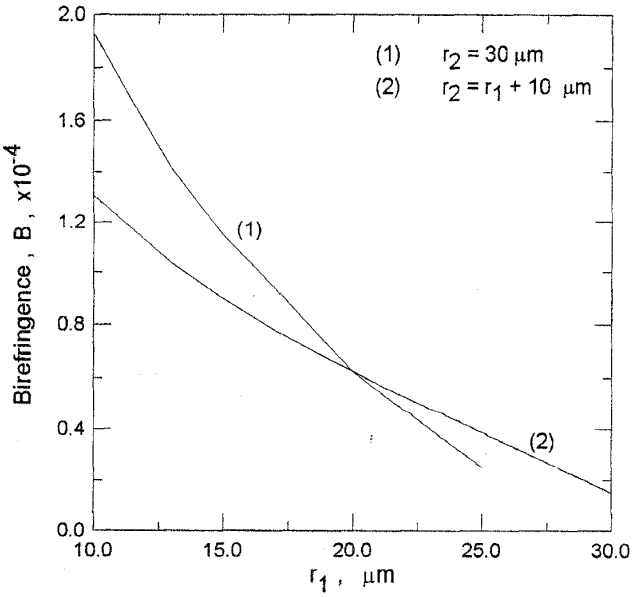

Fig. (9) Variation of the average birefringence, B, with respect to r_1, the inner radius of the SAZ, in a bow-tie fiber.

CONCLUSION:

The mechanical stress in both bow-tie and panda fibers has been calculated through the use of the thermoelastic potential method. The mechanical stress distribution has been used to

investigate the thermal-stress-induced birefringence for the two fiber types. The birefringence is found to be almost independent of the thermal expansion coefficient of the core material; however, the birefringence is dependent on the thermal expansion coefficient of both cladding and SAZ materials. The dimensions of the geometric structure of such fibers also contribute to the nature of the birefringence as follows: A higher birefringence can be achieved with a fiber with a larger cladding diameter, a larger SAZ area and a smaller distance of the SAZ from the center of the core. The axial stress, which is an important factor in designing an optical fiber, has been also calculated at different points in the fiber cross section. The adopted method can be applied successfully to fibers with any SAZ structure as well as those fibers with noncircular core.

REFERENCES

[1] C. A Villarruel, M. Abebe and W. Burns, "Birefringence Correction for Single-mode Fiber Couplers", Optical Letters, Vol. 7, No. 12, pp. 626-629, 1982.

[2] Allan W. Snyder and John D. Love, Optical Waveguide Thory, 1st ed., Chpman and Hall Ltd., 1983.

[3] John M. Senior, Optical Fiber Communications: Principles and Practice, 2nd ed., Printice Hall International Ltd, 1992.

[4] Katsunari Okamoto and Juichi Noda, "High-Birefringence Polarizing Fiber with Flat Cladding", IEEE J. Lightwave Technol., LT-3(4), pp. 758-762, 1985

[5] Danny Wong and Pak Lim Chu, "Stress Calculations Based on Point-Matching Method for Mechanically Inhomogeneous Optical Fibers", IEEE J. Lightwave Technol., LT-9(1), pp. 37-47, 1991.

[6] Pak L. Chu and Rowland A. Sammut, "Analytical method for Calculation of Stresses and Material Birefringence in Polarization-Maintaining Optical Fiber", IEEE J. Lightwave Technol., LT-2(5), pp. 650-662, 1984.

[7] Viliam Bernat and Alexander L. Yarin, "Analytical Solution for Stresses and Material Birefringence in Optical Fibers with Noncircular Cladding", IEEE J. Lightwave Technol., LT-10(4), pp. 413-417, 1992.

[8] Yueai Liu, B. M. A. Rahman and K.T. V. Grattan, "Analysis of the Birefringence Properties of Optical Fiber made by a Preform Deformation Technique", IEEE J. Lightwave Technol., LT-13(2), pp. 142-147, 1995.

[9] Juichi Noda and Yutaka Sasaki, "Polarization-Maintaining Fibers and Their Applications", IEEE J. Lightwave Technol., LT-4(8), pp. 1071-1089, 1986.

[10] S. P. Timoshenko and J. N. Goodier, Theory of Elasticity, 3rd ed., New York: McGraw-Hill, 1970.

[11] Kazuya Hayata and Michio Suzuki, " Stress-Induced Birefringence of Side-Tunnel Type Polarization-Maintaining Fibers", IEEE J. Lightwave Technol., LT-4(6), pp. 601-607, 1986.

[12] Ivan P. Kaminow, "Polarization in Optical Fibers", IEEE J. Quantum Electronics, QE-17(1), pp. 15-22, 1981.

[13] Yueai Liu and K. T. V. Grattan, "Thermal-Stress-Induced Birefringence in Bow-Tie Optical Fibers", J. Applied Optics, Vol. 33(24), pp. 5611-5616, 1994.

[14] Alfred E. Puro and Kalle-Juri E. Kell, "Complete Determination of Stress in fiber Preforms of Arbitrary Cross Section", IEEE J. Lightwave Technol., LT-10(8), pp. 1010-1014, 1992.